

First-order spatial coherence of excitons in planar nanostructures: a k_{\parallel} -filtering effect

L. Mouchliadis and A. L. Ivanov

Department of Physics and Astronomy, Cardiff University,

Queens Buildings, CF24 3AA, Cardiff, UK

(Dated: March 22, 2019)

Abstract

We propose and analyze a k_{\parallel} -filtering effect which gives rise to the drastic difference between the actual spatial coherence length of quasi-two-dimensional (quasi-2D) excitons or microcavity (MC) polaritons in planar nanostructures and that inferred from far-field optical measurements. The effect originates from the conservation of in-plane wavevector k_{\parallel} in the optical decay of the particles in outgoing bulk photons. The k_{\parallel} -filtering effect explains the large coherence lengths recently observed for indirect excitons in coupled quantum wells (QWs), but is less pronounced for MC polaritons at low temperatures, $T \lesssim 10$ K.

PACS numbers: 42.50.Ar, 78.67.De, 71.35.-y

Long-range spatial coherence is a fingerprint of well-developed Bose-Einstein (BE) statistics. Measurements of the first-order spatial coherence function $g^{(1)}$ and the coherence length ξ have allowed to visualize the BE condensation transition in a trapped Bose gas of Rb atoms¹. There are several recent reports on the observation of long-range spatial optical coherence in a low-temperature quasi-2D system of microcavity polaritons^{2,3} and indirect excitons^{4,5,6,7}. In this case, the resonant optical decay of MC polaritons or QW excitons in bulk photon modes allows to map the in-plane coherence function $g^{(1)}$ of the particles, by measuring the optical coherence function $\tilde{g}^{(1)}$ of the emitted photons. It is commonly assumed that the coherence length of QW excitons (MC polaritons), ξ_x (ξ_p), associated with $g^{(1)}$, is identical to that, ξ_γ , of the optical coherence function $\tilde{g}^{(1)}$.

In this Letter, we report a k_{\parallel} -filtering effect, which can strongly influence the optical coherence function $\tilde{g}^{(1)}$ measured from a planar nanostructure, and calculate $g^{(1)}$ and $\tilde{g}^{(1)}$ for QW excitons and MC polaritons. For QW excitons, the k_{\parallel} -filtering effect tremendously increases the optical coherence length ξ_γ , leading to $\xi_\gamma \gg \xi_x$, and can naturally explain the μm coherence lengths observed for indirect excitons and attributed to spontaneously developed coherence. The effect is less pronounced for MC polaritons, still with $\xi_\gamma \gtrsim \xi_p$.

The k_{\parallel} -filtering effect stems from the energy and in-plane momentum $\hbar k_{\parallel}$ conservation in the resonant conversion “quasi-2D QW exciton (MC polariton) \rightarrow outgoing bulk photon”. For a (coupled) quantum well surrounded by thick co-planar barrier layers, the case illustrated in Fig. 1, only low energy optically-active excitons from the radiative zone $k_{\parallel} \leq k_0 = (\sqrt{\varepsilon_b}/c)\omega_0$, with ε_b the dielectric constant of (AlGaAs) barrier layers and $\hbar\omega_0$ the exciton energy at $k_{\parallel} = 0$, are bright, i.e., can emit far-field light^{8,9,10}. In a far-field optical experiment with the detection angle 2α [see Fig. 1 (b)], the fraction of QW excitons which contribute to the optical signal is drastically reduced further to the wavevector band Δk_{\parallel} given by $0 \leq k_{\parallel} \leq k_{\parallel}^{(\alpha)} = (k_0/\sqrt{\varepsilon_b}) \sin \alpha \ll k_0$. The α -dependent narrowing of the detected states results in an effective broadening of the first-order spatial coherence function $\tilde{g}^{(1)}$. In addition, the sharp cutoff of the detected states at $k_{\parallel} = k_{\parallel}^{(\alpha)}$ yields an unusual oscillatory behavior of $\tilde{g}^{(1)}$. The k_{\parallel} -filtering effect has no analogy in optics of bulk excitons or polaritons.

The first-order spatial coherence function $g^{(1)}$ [11,12] of quantum well excitons, at a fixed time, is given by $g^{(1)}(\mathbf{r}'_{\parallel}, \mathbf{r}''_{\parallel}) = G^{(1)}(\mathbf{r}'_{\parallel}, \mathbf{r}''_{\parallel})/[G^{(1)}(\mathbf{r}'_{\parallel}, \mathbf{r}'_{\parallel})G^{(1)}(\mathbf{r}''_{\parallel}, \mathbf{r}''_{\parallel})]^{1/2}$ with $G^{(1)}(\mathbf{r}'_{\parallel}, \mathbf{r}''_{\parallel}) = \langle \hat{\Psi}^\dagger(\mathbf{r}'_{\parallel}) \hat{\Psi}(\mathbf{r}''_{\parallel}) \rangle$, where $\hat{\Psi}(\mathbf{r}'_{\parallel}) = (1/\sqrt{S}) \sum_{\mathbf{k}_{\parallel}} e^{i\mathbf{k}_{\parallel}\mathbf{r}'_{\parallel}} B_{\mathbf{k}_{\parallel}}$, \mathbf{r}_{\parallel} is the in-plane coordinate, S is the

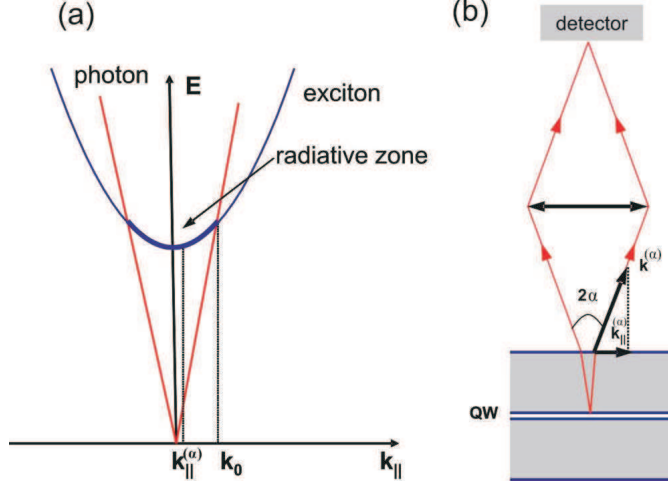


FIG. 1: (color online) Schematic of the k_{\parallel} -filtering effect. (a) The exciton and photon dispersions. Only low-energy QW excitons from the radiative zone $k_{\parallel} \leq k_0$ can emit outgoing bulk photons. (b) A far-field optical experiment with the detection angle 2α : A small fraction of QW excitons with $|k_{\parallel}| \leq k_{\parallel}^{(\alpha)} = (k_0/\sqrt{\varepsilon_b}) \sin \alpha$ contributes to the optical signal.

area, and $B_{\mathbf{k}_{\parallel}}$ is the exciton operator. Thus for isotropically distributed QW excitons one receives:

$$g^{(1)} = g^{(1)}(r_{\parallel}) = \frac{1}{2\pi n_{2d}} \int_0^{\infty} J_0(k_{\parallel} r_{\parallel}) n_{k_{\parallel}} k_{\parallel} dk_{\parallel}, \quad (1)$$

where $r_{\parallel} = |\mathbf{r}_{\parallel}'' - \mathbf{r}_{\parallel}'|$, n_{2d} is the concentration of particles, $n_{\mathbf{k}_{\parallel}} = \langle B_{\mathbf{k}_{\parallel}}^{\dagger} B_{\mathbf{k}_{\parallel}} \rangle$ is the occupation number, and J_0 is the zeroth-order Bessel function of the first kind. For a classical gas of QW excitons at thermal equilibrium, Eq.(1), with $n_{\mathbf{k}_{\parallel}}$ given by the Maxwell-Boltzmann (MB) distribution function $n_{k_{\parallel}}^{\text{MB}}$, yields the well-known result:

$$g^{(1)} = g_{\text{cl}}^{(1)}(r_{\parallel}) = e^{-\pi r_{\parallel}^2 / \lambda_{\text{dB}}^2}, \quad (2)$$

where the thermal de Broglie wavelength is given by $\lambda_{\text{dB}} = [(2\pi\hbar^2)/(M_x k_B T)]^{1/2}$ with T the temperature and M_x the exciton in-plane translational mass. For helium temperatures, one estimates from Eq. (2) the coherence length of MB-distributed indirect excitons in coupled QWs as $\xi_x \sim \lambda_{\text{dB}} \sim 0.1 \mu\text{m}$.

Comparing with Eq.(1), the spatial coherence function $\tilde{g}^{(1)}$ of photons emitted by QW excitons is given by

$$\tilde{g}^{(1)}(r_{\parallel}) = \frac{\int_0^{\infty} G_f(k_{\parallel}) J_0(k_{\parallel} r_{\parallel}) n_{k_{\parallel}} k_{\parallel} dk_{\parallel}}{\int_0^{\infty} G_f(k_{\parallel}) n_{k_{\parallel}} k_{\parallel} dk_{\parallel}}, \quad (3)$$

where $G_f = \Theta(k_{\parallel}^{(\alpha)} - k_{\parallel})\Gamma_{x-\gamma}(k_{\parallel})$ is the k_{\parallel} -filtering function with $\Theta(x)$ the step function and $\Gamma_{x-\gamma}(k_{\parallel})$ the efficiency of the resonant conversion of a QW exciton in an outgoing bulk photon. The function G_f reduces the integration limits on the right-hand side (r.h.s.) of Eq. (3) to the narrow band $\Delta k_{\parallel} = [0, k_{\parallel}^{(\alpha)}]$ and describes the k_{\parallel} -filtering effect in high-quality planar nanostructures. If both the function $\Gamma_{x-\gamma}(k_{\parallel})$ and the occupation number $n_{k_{\parallel}}$ do not change significantly in the narrow band Δk_{\parallel} , Eq. (3) yields:

$$\tilde{g}^{(1)} = \tilde{g}_f^{(1)}(r_{\parallel}) = 2J_1(k_{\parallel}^{(\alpha)} r_{\parallel}) / (k_{\parallel}^{(\alpha)} r_{\parallel}), \quad (4)$$

where J_1 is the first-order Bessel function of the first kind. From Eq. (4) one concludes that the optical coherence length ξ_{γ} , evaluated as the half width at half maximum of $\tilde{g}^{(1)} = \tilde{g}_f^{(1)}(r_{\parallel})$, is given by

$$4J_1(k_{\parallel}^{(\alpha)} \xi_{\gamma}) = k_{\parallel}^{(\alpha)} \xi_{\gamma} \rightarrow k_{\parallel}^{(\alpha)} \xi_{\gamma} \simeq 2.215. \quad (5)$$

Equations (4)-(5) illustrate the net k_{\parallel} -filtering effect: $\xi_{\gamma} \propto 1/k_{\parallel}^{(\alpha)} \propto 1/\sin \alpha$ strongly increases with decreasing aperture angle 2α . Below we analyze in more detail the polarization function $g^{(1)}$ against the optical $\tilde{g}^{(1)}$, assuming no phase transition to a collective (superfluid) quasi-2D state¹³.

First-order spatial coherence of non-interacting quasi-2D bosons (excitons) in equilibrium. In this case, the chemical potential μ_{2d} is given by $\mu_{2d}^{(0)} = k_B T \ln(1 - e^{-T_0/T})$ with $k_B T_0 = (2\pi/g)(\hbar^2/M_x)n_{2d}$ the quantum degeneracy temperature and g the spin degeneracy factor of bosons ($g = 4$ for indirect excitons). By substituting $n_{\mathbf{k}_{\parallel}} = n_{\mathbf{k}_{\parallel}}^{\text{BE}}$ into Eq. (1), where $n_{\mathbf{k}_{\parallel}}^{\text{BE}}$ is the Bose-Einstein occupation number, one receives:

$$\begin{aligned} g^{(1)} &= g_{\text{hint}}^{(1)}(r_{\parallel}) = \frac{T}{T_0} g_1(1 - e^{T_0/T}, e^{-\pi r_{\parallel}^2/\lambda_{\text{dB}}^2}) \\ &= \frac{T}{T_0} \sum_{n=1}^{\infty} \frac{(1 - e^{-T_0/T})^n}{n} e^{-\pi r_{\parallel}^2/n\lambda_{\text{dB}}^2}. \end{aligned} \quad (6)$$

Here, the generalized Bose function[?] $g_{\alpha}(x, y)$ with $\alpha = 1$ is defined as $g_{\alpha}(x, y) = \sum_{k=1}^{\infty} (x^k y^{1/k})/k^{\alpha}$.

For small distances, $r_{\parallel} \ll \lambda_{\text{dB}}$, Eq. (6) yields:

$$g^{(1)}(r_{\parallel} \ll \lambda_{\text{dB}}) \simeq 1 - \frac{T}{T_0} \frac{\pi r_{\parallel}^2}{\lambda_{\text{dB}}^2} \text{Li}_2(1 - e^{-T_0/T}), \quad (7)$$

where $\text{Li}_{\alpha}(x) = \sum_{k=1}^{\infty} x^k/k^{\alpha}$ with $\alpha = 2$ is the polylogarithm. For $T \gg T_0$, Eq. (7) recovers the classical limit, $g_{\text{cl}}^{(1)}(r_{\parallel} \rightarrow 0) \simeq 1 - (\pi r_{\parallel}^2)/\lambda_{\text{dB}}^2$, which is consistent with Eq. (2). For large

distances, $r_{\parallel} \gtrsim r_{\parallel}^{(q)} = \lambda_{\text{dB}} [- (2/\pi) \ln(1 - e^{-T_0/T})]^{1/2}$, Eq. (6) reduces to

$$g^{(1)}(r_{\parallel} \gtrsim r_{\parallel}^{(q)}) \simeq 2 \frac{T}{T_0} K_0 \left(\frac{r_{\parallel}}{r_0} \right), \quad (8)$$

where K_0 is the modified Bessel function of the second kind and $r_0 = \lambda_{\text{dB}} / [-4\pi \ln(1 - e^{-T_0/T})]^{1/2}$. Equation (8) explicitly includes quantum corrections to the first-order correlation function $g^{(1)}$, through $T_0 \propto \hbar^2$. For $r_{\parallel} \gg r_0$, Eq. (8) reduces further to the quantum limit:

$$g^{(1)} = g_{\text{q}}^{(1)}(r_{\parallel} \gg r_0) = \sqrt{2\pi} \frac{T}{T_0} \sqrt{\frac{r_0}{r_{\parallel}}} e^{-r_{\parallel}/r_0}. \quad (9)$$

For temperatures $T \gg T_0$, the spatial coherence function is well approximated by Eq. (2), and the quantum corrections given by Eq. (9) refer to large $r_{\parallel} \gtrsim \lambda_{\text{dB}} \sqrt{(2/\pi) \ln(T/T_0)} \gg \lambda_{\text{dB}}$, and, therefore, to very small values of $g^{(1)}$. The latter conclusion is consistent with the $e^{-\pi r_{\parallel}^2/n\lambda_{\text{dB}}^2}$ - series on the r.h.s. of Eq. (6). For $T \lesssim T_0$, when Bose-Einstein statistics is well-developed, Eq. (9) is valid for distances larger than $\lambda_{\text{dB}} \sqrt{(2/\pi)} e^{-T_0/2T} \ll \lambda_{\text{dB}}$, so that $g^{(1)}$ is well-approximated by $g_{\text{q}}^{(1)}$ for any r_{\parallel} .

Thus, with temperature T decreasing from $T \gg T_0$ to $T \lesssim T_0$, the coherence function $g^{(1)}$ changes from the $n_{2\text{d}}$ -independent Gaussian $g_{\text{cl}}^{(1)}(r_{\parallel})$, given by Eq. (2), to the $n_{2\text{d}}$ -dependent exponentially decaying $g_{\text{q}}^{(1)}(r_{\parallel})$, given by Eq. (9). The quantum statistical effects considerably increase the correlation length ξ_x , as shown in Fig. 2. For $T \lesssim T_0$ one has $\xi_x \sim r_0 \simeq [\lambda_{\text{dB}} / (2\sqrt{\pi})] e^{T_0/2T}$, i.e., ξ_x increases exponentially with increasing density $n_{2\text{d}}$. This is due to large population of the low-energy states, in particular the ground-state mode $\mathbf{k}_{\parallel} = 0$: $n_{\mathbf{k}_{\parallel}=0}^{\text{BE}} = e^{T_0/T} - 1$.

The coherence function $g^{(1)}$ of weakly-interacting thermal QW excitons. For circularly polarized excitons in a single quantum well, the case relevant to MC polaritons, the repulsive interaction between the particles is well approximated by a contact potential $U_{\text{sqw}} = (u_0/2)\delta(\mathbf{r}_{\parallel})$ with $u_0 = u_0^{\text{sqw}} > 0$. In this case, the mean-field (Hartree-Fock) interaction only shifts the chemical potential, $\mu_{2\text{d}} = \mu_{2\text{d}}^{(0)} + u_0^{\text{sqw}} n_{2\text{d}}$, leaving unchanged Eqs. (6)-(9) for the coherence function $g^{(1)}$.

For indirect excitons in coupled QWs, the mid-range dipole-dipole repulsive interaction U_{cqw} of the particles cannot be generally approximated by a contact potential. Following [15], we use the two-parametric model potential $U_{\text{cqw}}(r_{\parallel}) = [(\sqrt{\pi}u_0w)/r_{\parallel}^3] (1 - e^{-r_{\parallel}^2/w^2})$ with parameters $u_0 = u_0^{\text{cqw}} \simeq 4\pi(e^2/\varepsilon_{\text{b}})d_z$ [16,17] and $w \simeq a_{\text{x}}^{(2\text{d})}$, where ε_{b} is the static dielectric con-

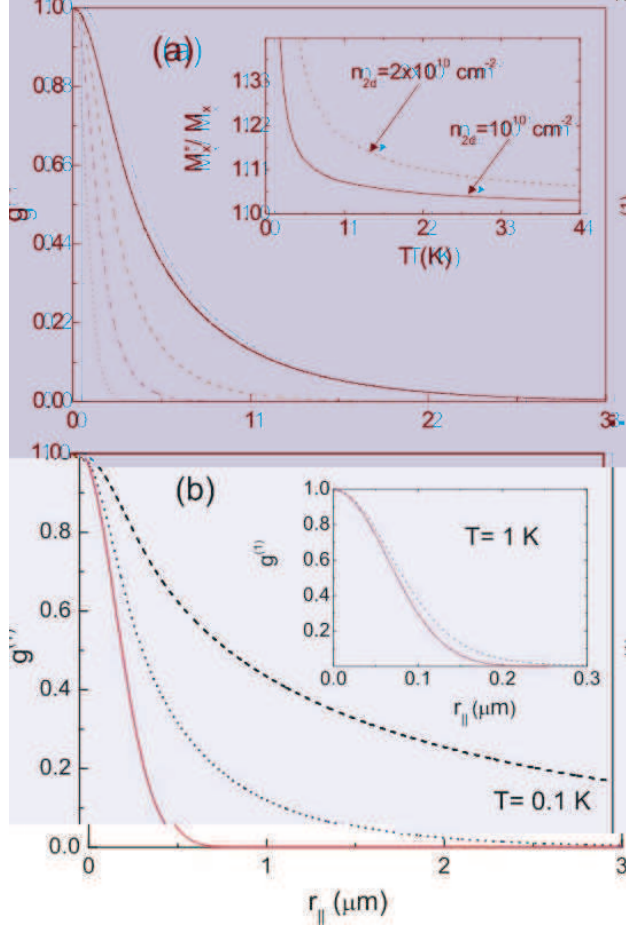


FIG. 2: (color online) (a) The first-order spatial coherence function $g^{(1)} = g_{\text{ind}}^{(1)}(r_{\parallel})$ of indirect excitons in a GaAs coupled QW structure with $d_z = 11.5$ nm and $w = 15$ nm: $n_{2d} = 10^{10} \text{ cm}^{-2}$ and $T = 1$ K (dotted line), 0.4 K (dash-dotted line), 0.2 K (dashed line), and 0.1 K (solid line). Inset: The renormalized mass M_x^* against temperature T , calculated with Eq. (11) for $n_{2d} = 10^{10} \text{ cm}^{-2}$ (solid line) and $2 \times 10^{10} \text{ cm}^{-2}$ (dashed line). (b) $g^{(1)} = g_{\text{cl}}^{(1)}(r_{\parallel})$ calculated with Eq. (2) (solid line), $g^{(1)} = g_{\text{nint}}^{(1)}(r_{\parallel})$ evaluated with Eq. (6), and $g^{(1)} = g_{\text{ind}}^{(1)}(r_{\parallel})$ calculated with Eqs. (6), (10) and (11) (dotted line): $n_{2d} = 10^{10} \text{ cm}^{-2}$ and $T = 0.1$ K. Inset: the same functions evaluated for $n_{2d} = 10^{10} \text{ cm}^{-2}$ and $T = 1$ K.

stant, d_z is the distance between coupled quantum wells, and $a_x^{(2d)}$ is the radius of an indirect exciton. The model potential reproduces $1/r_{\parallel}^3$ behavior at $r_{\parallel} \gtrsim a_x^{(2d)}$ and $1/r_{\parallel}$ Coulomb repulsive potential at $r_{\parallel} \lesssim a_x^{(2d)}$. The self-consistent Hartree-Fock (HF) analysis¹⁸ of the Hamiltonian $H_x = \sum_{\mathbf{p}_{\parallel}} [(\hbar^2 p_{\parallel}^2)/(2M_x)] B_{\mathbf{p}_{\parallel}}^{\dagger} B_{\mathbf{p}_{\parallel}} + 1/(2S) \sum_{\mathbf{p}_{\parallel}, \mathbf{l}_{\parallel}, \mathbf{q}_{\parallel}} U_{\text{cqw}}(\mathbf{q}_{\parallel}) B_{\mathbf{p}_{\parallel}}^{\dagger} B_{\mathbf{l}_{\parallel}}^{\dagger} B_{\mathbf{l}_{\parallel} + \mathbf{q}_{\parallel}} B_{\mathbf{p}_{\parallel} - \mathbf{q}_{\parallel}}$ yields the n_{2d} - and T -dependent change of the in-plane translational mass M_x . In this case, μ_{2d} is

given by

$$\begin{aligned} \mu_{2d} = & \mu_{2d}^{(0)} + u_0 n_{2d} + \frac{u_0}{2(\lambda_{\text{dB}}^*)^2} \left[\frac{T_0^*}{T} + \sqrt{\pi} \frac{w}{\lambda_{\text{dB}}^*} \right. \\ & \left. \times \left[\frac{\sqrt{\pi}}{2} \frac{w}{\lambda_{\text{dB}}^*} \text{Li}_2(1 - e^{-T_0^*/T}) - \text{Li}_{3/2}(1 - e^{-T_0^*/T}) \right] \right], \end{aligned} \quad (10)$$

where, alongside Eq. (6), both the de Broglie wavelength λ_{dB}^* and the degeneracy temperature T_0^* are changed according to $M_x \rightarrow M_x^*$. The particle mass M_x^* renormalized by the dipole-dipole interaction is given as a single solution of the transcendental equation:

$$\frac{1}{M_x^*} = \frac{1}{M_x} + \frac{u_0 w}{8\sqrt{\pi}\hbar^2\lambda_{\text{dB}}^*} \left[\sqrt{\pi} \frac{w}{\lambda_{\text{dB}}^*} \frac{T_0^*}{T} - \text{Li}_{1/2}(1 - e^{-T_0^*/T}) \right]. \quad (11)$$

In Fig. 2 (a) we plot $g^{(1)} = g_{\text{ind}}^{(1)}(r_{\parallel})$ evaluated numerically by using Eqs. (6), (10) and (11) for indirect excitons in a GaAs coupled QW structure. In Fig. 2 (b), the coherence function $g_{\text{ind}}^{(1)}$ is compared with $g_{\text{cl}}^{(1)}$ evaluated with Eq. (2) and $g_{\text{nint}}^{(1)}$ calculated with Eq. (6) for non-interacting excitons. The main result is that the dipole-dipole repulsive interaction induces an increase of the translational mass [see the inset of Fig. 2 (a), note that the applied self-consistent HF approximation becomes invalid when $\Delta M_x = M_x^* - M_x \gtrsim M_x$] and, therefore, decreases the coherence length ξ_x comparing to that of non-interacting particles [see also Fig. 3 (a)]. The effect, however, becomes visible only at temperatures well below 1 K. For $T = 1$ K all three correlation functions, $g_{\text{ind}}^{(1)}$, $g_{\text{cl}}^{(1)}$, and $g_{\text{nint}}^{(1)}$, nearly coincide, as is clearly seen in the inset of Fig. 2 (b). In other words, for $n_{2d} \sim 10^{10} \text{ cm}^{-2}$ and $T \gtrsim 1.5$ K, which are relevant to the experiments^{4,5,6,7}, the quantum limit, i.e., $g^{(1)} = g_{\text{q}}^{(1)}$ given by Eq. (9), cannot build up. For example, for $n_{2d} = 10^{10} \text{ cm}^{-2}$ and $T = 1.5$ K one estimates $T_0 \simeq T_0^* \simeq 0.65$ K and $n_{k_{\parallel}=0}^{\text{BE}} \simeq 0.54 < 1$, so that BE statistics is rather weakly developed to influence the coherence length ξ_x .

The optical spatial coherence function $\tilde{g}^{(1)}$ of indirect excitons. In order to explain the experiments^{4,5,6,7}, which demonstrate a coherence length ξ_{γ} much larger than $\xi_x \sim 0.1 \mu\text{m}$, we implement the concept of k_{\parallel} -filtering. In this case, $\tilde{g}^{(1)} = \tilde{g}_{\text{ind}}^{(1)}(r_{\parallel})$ is given by Eq. (3) with the efficiency of the “indirect exciton \rightarrow bulk photon” conversion $\Gamma_{x-\gamma} = (2k_0^2 - k_{\parallel}^2)/[k_0(k_0^2 - k_{\parallel}^2)^{1/2}]$ [8,9,10,19]. In Fig. 3 (b), we plot $\tilde{g}_{\text{ind}}^{(1)}$ calculated for various aperture angles, $2^\circ \lesssim 2\alpha \lesssim 40^\circ$. The dependence $\tilde{g}^{(1)} = \tilde{g}_{\text{ind}}^{(1)}(r_{\parallel})$ is well-approximated by Eq. (4). The above approximation of $\tilde{g}^{(1)}$ by the “device function” $\tilde{g}_{\text{f}}^{(1)}$ is valid when $n_{k_{\parallel}} = n_{E=\hbar^2 k_{\parallel}^2/2M_x}^{\text{BE}}$ is

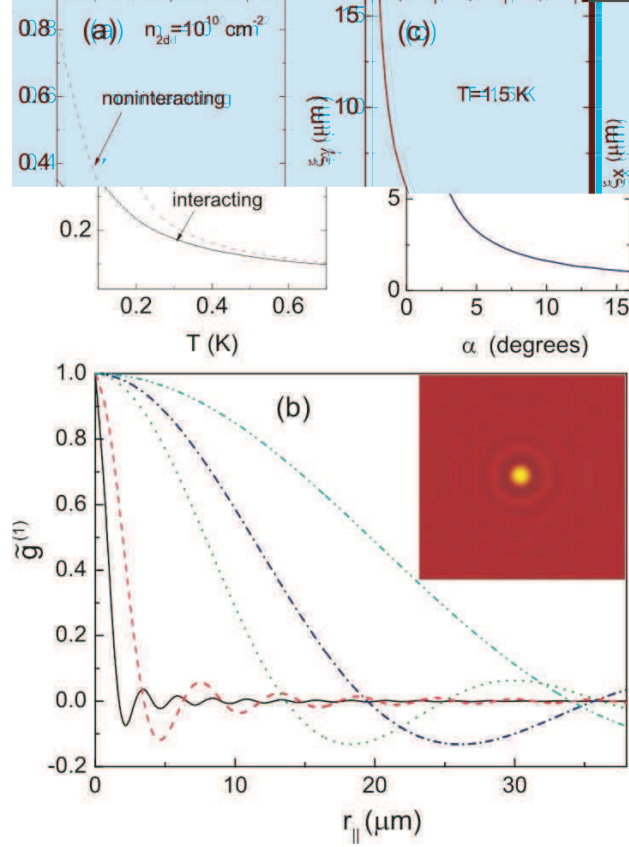


FIG. 3: (color online) (a) The dependence of the correlation length ξ_x against temperature T , calculated for noninteracting (dashed line) and dipole-dipole interacting (solid line) indirect excitons. (b) The k_{\parallel} -filtering effect: $\tilde{g}^{(1)} = \tilde{g}^{(1)}(r_{\parallel})$ evaluated for $\alpha = 18.9^\circ$ (solid line), 8.3° (dashed line), 2.1° (dotted line), 1.4° (dashed-dotted line), and 0.8° (dashed-double-dotted line). Inset: The real-space 2D image of $\tilde{g}^{(1)}$. (c) The coherence length ξ_γ against the aperture angle 2α .

nearly constant in the rather narrow energy interval $0 \leq E \leq E^{(\alpha)}$, i.e., when

$$E^{(\alpha)} = (\hbar k_{\parallel}^{(\alpha)})^2 / 2M_x \ll k_B T e^{-T_0/T}. \quad (12)$$

For indirect excitons, the inequality (12) with T_0 replaced by T_0^* is definitely held for $n_{2d} \sim 10^{10} \text{ cm}^{-2}$ and $T \sim 1 \text{ K}$ (e.g., for $\alpha = 20^\circ$ the cutoff energy $E^{(\alpha)}$ is only $1.2 \mu\text{eV}$). Thus the k_{\parallel} -filtering effect yields the correlation length $\xi_\gamma \simeq 2.215 \sqrt{\epsilon_b} / (k_0 \sin \alpha)$ with $k_0 \simeq 2.8 \times 10^5 \text{ cm}^{-1}$, according to Eq. (5). As a result, ξ_γ is intrinsically scaled by the photon wavelength, i.e., is in the μm length scale [see Fig. 3 (c), where ξ_γ is plotted against the angle α].

Comparing to standard interference patterns in Young's double-slit experiment, with contrast determined by $\tilde{g}^{(1)}$, the oscillatory behavior of the optical coherence function $\tilde{g}^{(1)} =$

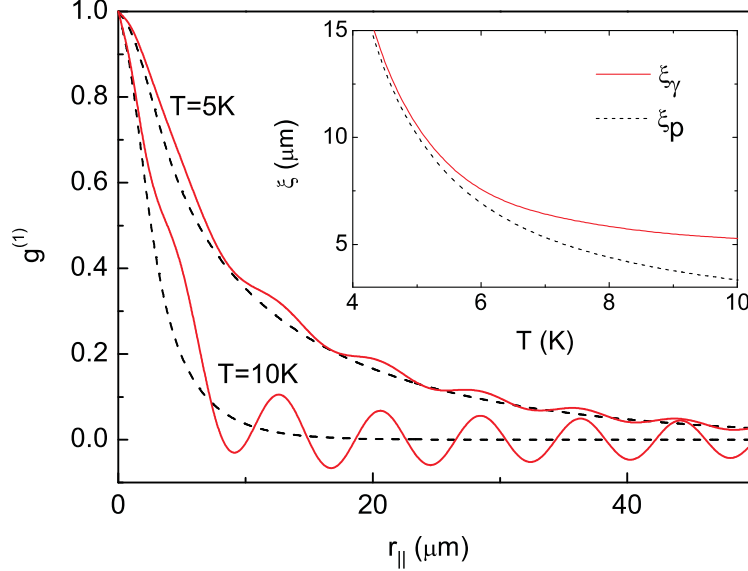


FIG. 4: (color online) The MC polariton coherence function $g^{(1)} = g_{\text{MC}}^{(1)}(r_{\parallel})$ (dashed lines) against that of emitted photons, $\tilde{g}^{(1)} = \tilde{g}_{\text{MC}}^{(1)}(r_{\parallel})$ (solid lines). Inset: The coherence lengths ξ_{p} and ξ_{γ} versus temperature T . The calculations, which model the experiments², refer to a GaAs microcavity with positive detuning $\delta = 7$ meV and Rabi splitting $\Omega_{\text{MC}} = 4$ meV. The density of MC polaritons $n_{2\text{d}} = 10^8 \text{ cm}^{-2}$ and the aperture half-angle $\alpha = 16.7^\circ$, so that $T_0 = 27.6$ K and $E^{(\alpha)} = 0.96$ meV.

$\tilde{g}^{(1)}(r_{\parallel})$ is rather unusual [see Eq. (4) and Fig. 3 (b)]. This is a signature of the k_{\parallel} -filtering effect: The k_{\parallel} -filtering function $G_{\text{f}} \propto \Theta(k_{\parallel}^{(\alpha)} - k_{\parallel})$ gives a sharp cutoff at $k_{\parallel} = k_{\parallel}^{(\alpha)}$ in the integrals of Eq. (3) that results in oscillations of $\tilde{g}^{(1)}(r_{\parallel})$. In some aspects, the effect is similar to Friedel oscillations in a Fermi liquid, with $\hbar k_{\parallel}^{(\alpha)}$ akin to the Fermi momentum.

The coherence function $\tilde{g}^{(1)}$ of MC polaritons. In this case, the ‘‘MC polariton \rightarrow bulk photon’’ conversion function in Eq. (3) is $\Gamma_{\text{x}\rightarrow\gamma} = \Psi(k_{\parallel})/\tau_{\gamma}(k_{\parallel})$ with Ψ ($0 \leq \Psi \leq 1$) the photon component along a MC polariton branch and τ_{γ} the radiative (escape) lifetime of a MC photon. In Fig. 4, $g^{(1)} = g_{\text{MC}}^{(1)}(r_{\parallel})$ calculated with Eq. (6) for circularly polarized MC polaritons is compared with $\tilde{g}^{(1)} = \tilde{g}_{\text{MC}}^{(1)}(r_{\parallel})$ evaluated with Eq. (3). According to the experiments^{2,3}, we assume the BE distribution of MC polaritons along the lower polariton branch which is taken in the parabolic approximation with an effective in-plane mass $M_{\text{MC}}^{\text{lb}}$. Comparing to the case of QW excitons, the difference between $g_{\text{MC}}^{(1)}$ and $\tilde{g}_{\text{MC}}^{(1)}$ is much smaller, still giving $\xi_{\gamma} > \xi_{\text{p}}$. This is because the cutoff energy $E^{(\alpha)}$ in the k_{\parallel} -filtering effect is much larger than that relevant to QW excitons [in Eq. (12) M_{x} should be replaced by $M_{\text{MC}}^{\text{lb}} \ll M_{\text{x}}$]. The functions $g_{\text{MC}}^{(1)}$ and $\tilde{g}_{\text{MC}}^{(1)}$ nearly coincide, if $k_{\text{B}}T \ll E^{(\alpha)}$ (see Fig. 4).

We qualitatively explain a sharp increase of the coherence length with decreasing temperature, found in the experiments with coupled QWs^{4,5,6,7}, by combining the k_{\parallel} -filtering effect with screening of disorder by dipole-dipole interacting indirect excitons¹⁷. In high-quality GaAs coupled QWs the screening process effectively develops at $T \lesssim 5$ K, giving rise to a well-defined single-particle momentum $\hbar\mathbf{k}_{\parallel}$, as has been observed, e.g., in the experiments^{20,21}. Thus the large correlation length $\xi = \xi_{\gamma} \sim 1 \mu\text{m}$, which strongly depends on α , can naturally be explained by the k_{\parallel} -filtering effect and can occur even for the Maxwell-Boltzmann distributed particles. In order to see an increase of ξ due to quantum statistics, the bath temperature should be decreased to tens of mK.

We appreciate valuable discussions with L. V. Butov.

-
- ¹ I. Bloch, T. W. Hänsch, and T. Eslinger, *Nature* **403**, 166 (2000).
- ² H. Deng, Glenn S. Solomon, R. Hey, K. H. Ploog, and Y. Yamamoto, *Phys. Rev. Lett.* **99**, 126403 (2007).
- ³ J. Kasprzak, M. Richard, S. Kundermann, A. Baas, P. Jeambrun, J. M. J. Keeling, F. M. Marchetti, M. H. Szymańska, R. André, J. L. Staehli, V. Savona, P. B. Littlewood, B. Deveaud, and Le Si Dang, *Nature* **443**, 409 (2006).
- ⁴ S. Yang, A. T. Hammack, M. M. Fogler, L. V. Butov, and A. C. Gossard, *Phys. Rev. Lett.* **97**, 187402 (2006).
- ⁵ A. V. Gorbunov and V. B. Timofeev, *Pis'ma Zh. Teor. Fiz.* **84**, 390 (2006) [*JETP Lett.* **84**, 329 (2006)].
- ⁶ L. V. Butov, *J. Phys. Condens. Matter* **19**, 295202 (2007).
- ⁷ V. B. Timofeev, in *Problems of Condensed Matter Physics* edited by A. L. Ivanov and S. G. Tikhodeev (OUP, Oxford, 2008), pp. 258-284.
- ⁸ E. Hanamura, *Phys. Rev. B* **38**, 1228 (1988).
- ⁹ L. C. Andreani, F. Tassone, and F. Bassani, *Solid State Commun.* **77**, 641 (1990).
- ¹⁰ D. Citrin, *Phys. Rev. B* **47**, 3832 (1993).
- ¹¹ R. J. Glauber, in *Quantum Optics and Electronics*, edited by C. DeWitt, A. Blandin, and C. Cohen-Tannoudji (Gordon and Breach Publishers, New York, 1965).
- ¹² M. O. Scully and M. S. Zubairy, *Quantum Optics* (Cambridge University Press, Cambridge,

- 1997).
- ¹³ P. N. Brusov and V. N. Popov, *Superfluidity and Collective Properties of Quantum Liquids* (Nauka, Moscow, 1988).
- ¹⁴ M. Narachewski and R. J. Glauber Phys. Rev. A **59**, 4595 (1999).
- ¹⁵ D. M. Kachintsev and S. E. Ulloa Phys. Rev. B **50**, 8715 (1994).
- ¹⁶ L. V. Butov, J. Phys. Condens. Matter **16**, R1577 (2004).
- ¹⁷ A. L. Ivanov, Europhys. Lett. **59**, 586 (2002); J. Phys. Condens. Matter **16**, S3629 (2004).
- ¹⁸ A. L. Fetter and J. D. Walecka, *Quantum Theory of Many-Particle Systems* (McGraw-Hill, New York, 1971).
- ¹⁹ A. L. Ivanov, P. B. Littlewood, and H. Haug, Phys. Rev. B **59**, 5032 (1999).
- ²⁰ A. Parlangeli, P. C. M. Christianen, J. C. Maan, I. V. Tokatly, C. B. Soerensen, and P. E. Lindelof, Phys. Rev. B **62**, 15323 (2000).
- ²¹ L. V. Butov, A. L. Ivanov, A. Imamoglu, P. B. Littlewood, A. A. Shashkin, V. T. Dolgoplov, K. L. Campman, and A. C. Gossard, Phys. Rev. Lett. **86**, 5608 (2001).